Journal of Advanced Research 45 (2023) 1–13

Contents lists available at ScienceDirect

Journal of Advanced Research

journal homepage: www.elsevier.com/locate/jare

Original Article

SCAP deficiency facilitates obesity and insulin resistance through shifting adipose tissue macrophage polarization

Jae-Ho Lee [a,1], Sun Hee Lee [a,1], Eun-Ho Lee [a], Jeong-Yong Cho [b], Dae-Kyu Song [a], Young Jae Lee [c], Taeg Kyu Kwon [d], Byung-Chul Oh [e], Kae Won Cho [f], Timothy F. Osborne [g], Tae-Il Jeon [h], Seung-Soon Im [a,*]

[a] Department of Physiology, Keimyung University School of Medicine, Daegu 42601, Republic of Korea
[b] Department of Food Science and Technology, Chonnam National University, Gwangju 61186, Republic of Korea
[c] Lee Gil Ya Cancer and Diabetes Institute, Department of Biochemistry, Gachon University School of Medicine, Younsoo-gu, Inchon 21999, Republic of Korea
[d] Department of Immunology, Keimyung University School of Medicine, Daegu 42601, Republic of Korea
[e] Lee Gil Ya Cancer and Diabetes Institute, Department of Physiology, Gachon University School of Medicine, Younsoo-gu, Inchon 21999, Republic of Korea
[f] Soonchunhyang Institute of Medi-bioScience (SIMS), Soonchunhyang University, Cheonan 31151, Republic of Korea
[g] Institute for Fundamental Biomedical Research, Departments of Medicine and Biological Chemistry, Johns Hopkins University School of Medicine, St. Petersburg, FL 33701, USA
[h] Department of Animal Science, College of Agriculture and Life Science, Chonnam National University, Gwangju 61186, Republic of Korea

HIGHLIGHTS

- Deletion of SCAP in macrophages increases the fat accumulation of HFHS from an increase in M1 Adipose tissue macrophages.
- Loss of SCAP reduces M2 macrophage polarization.
- SCAP-induced activation of SREBP-1a stimulates Ch25H gene expression in macrophages.
- The effects of SCAP deficiency in macrophages suppress cholesterol efflux and increase intracellular cholesterol crystal to induce HFHS-mediated M1 macrophage polarization.

GRAPHICAL ABSTRACT

Schematic model for SCAP in macrophage polarization of adipose tissue in metabolic diseases. *Introduction:*

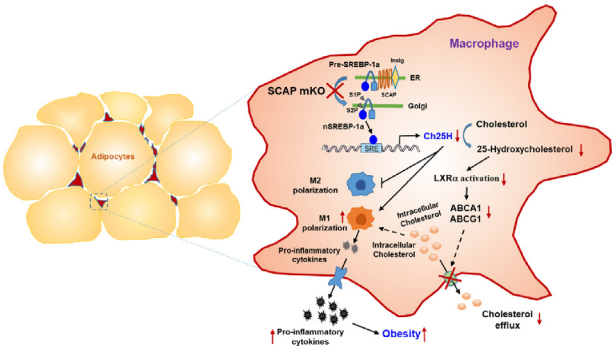

ARTICLE INFO

Article history:
Received 26 March 2022
Revised 13 May 2022
Accepted 26 May 2022
Available online 31 May 2022

Keywords:
SCAP
White adipose tissue
Macrophages
Cholesterol 25-hydroxylase
Cholesterol efflux

ABSTRACT

Introduction: Sterol regulatory element binding protein (SREBP) cleavage-associating protein (SCAP) is a sterol-regulated escort protein that translocates SREBPs from the endoplasmic reticulum to the Golgi apparatus, thereby activating lipid metabolism and cholesterol synthesis. Although SCAP regulates lipid metabolism in metabolic tissues, such as the liver and muscle, the effect of macrophage-specific SCAP deficiency in adipose tissue macrophages (ATMs) of patients with metabolic diseases is not completely understood.

Objectives: Here, we examined the function of SCAP in high-fat/high-sucrose diet (HFHS)-fed mice and investigated its role in the polarization of classical activated macrophages in adipose tissue.

Methods: Macrophage-specific SCAP knockout (mKO) mice were generated through crossbreeding lysozyme 2-cre mice with SCAP floxed mice which were then fed HFHS for 12 weeks. Primary macrophages were derived from bone marrow cells and analyzed further.

Peer review under responsibility of Cairo University.

* Corresponding author.
E-mail address: ssim73@kmu.ac.kr (S.-S. Im).

[1] Authors equally contributed to this study.

https://doi.org/10.1016/j.jare.2022.05.013

Results: We found that fat accumulation and the appearance of proinflammatory M1 macrophages were both higher in HFHS-fed SCAP mKO mice relative to floxed control mice. We traced the effect to a defect in the lipopolysaccharide-mediated increase in SREBP-1a that occurs in control but not SCAP mKO mice. Mechanistically, SREBP-1a increased expression of cholesterol 25-hydroxylase transcription, resulting in an increase in the production of 25-hydroxycholesterol (25-HC), an endogenous agonist of liver X receptor alpha (LXRα) which increased expression of cholesterol efflux to limit cholesterol accumulation and M1 polarization. In the absence of SCAP mediated activation of SREBP-1a, increased M1 macrophage polarization resulted in reduced cholesterol efflux downstream from 25-HC-dependent LXRα activation.

Conclusion: Overall, the activation of the SCAP-SREBP-1a pathway in macrophages may provide a novel therapeutic strategy that ameliorates obesity by controlling cholesterol homeostasis in ATMs.

Introduction

Fat accumulation is accompanied by the elevation of circulating proinflammatory cytokine levels and accumulation of adipose tissue macrophages (ATMs) [1,2]. Macrophages exhibit significant plasticity and can modify phenotypes and functions in response to tissue stress and inflammatory responses [3]. Generally, ATMs are classified as either the proinflammatory M1 or anti-inflammatory M2 phenotype [4,5]. Although this grouping does not consider the complexity and functional diversity of macrophages *in vivo,* the ratio of M1 to M2 ATMs correlates with the occurrence of metabolic syndromes, including obesity, diabetes, hepatic steatosis, and atherosclerosis in humans and mice [6,7]. Therefore, macrophage polarization and infiltration may be key events triggering the development of obesity-associated metabolic syndromes.

Sterol regulatory element binding protein (SREBP) cleavage-activating protein (SCAP) is involved in controlling triglyceride (TG) and cholesterol homeostasis via the regulation of SREBP movement from the endoplasmic reticulum to the Golgi apparatus [8]. Several studies in tissue-specific SCAP depleted mice have established critical functions of SCAP in various cells and tissues [9]. Though genetic deletion of SCAP markedly enhanced type 1 interferon response in macrophages through a decrease in flux through the sterol biosynthesis pathway [10], the effect of macrophage-specific SCAP knockout (SCAP mKO) has not been studied in metabolic dysregulation *in vivo*. Previously, SREBP-1a has been shown to be a predominant form of SREBP-1 in immune cells and is required for regulating the synthesis of inflammation-mediated unsaturated fatty acids in macrophages [11,12]. Furthermore, SREBP-1-deficient macrophages exhibited a hyper-inflammatory response to an increased expression of inflammatory cytokine-encoding genes, and exaggerated inflammatory states were induced by lipopolysaccharide (LPS) challenge in SREBP-1 KO mice, and this was accompanied by increased levels of plasma cytokines, such as interleukin (IL)-6 and IL-1α [11]. However, whether SCAP and SREBPs modulate ATM function during metabolic challenge has not been reported. Thus, a functional study of SCAP in the ATMs may help provide a connection between SREBP function in immune cells and tissue selective contributions to metabolic syndrome disorders.

Previous studies have demonstrated that the accumulation of intracellular cholesterol crystals generally induces proinflammatory responses and macrophage infiltration in tissues [13,14]. In particular, oxysterol 25-hydroxycholesterol (25-HC), among produced cholesterols, suppresses IL-1-induced proinflammatory responses [15]. Cholesterol 25-hydroxylase (Ch25H) plays an important role in converting cholesterol to 25-HC in macrophages [16], which is involved in immune responses and contributes to the anti-inflammatory response via the repression of inflammasome activity. In adipose tissue, *Ch25H* was identified as a member of the macrophage-enriched metabolic network [17]. Along with 25-HC, it functions via the activation of the Toll-like receptor (TLR) [18–20], interferon receptor (IFNR) [21], and liver X receptor (LXR) [22] in macrophages, indicating that Ch25H links metabolic signaling to inflammatory responses. Previous study with *Ch25H* KO mice has revealed its protective effect during inflammatory responses and the subsequent reduction in the severity of pulmonary lesions [19]. However, although its functional regulation has been revealed in various tissues, such as in the liver, lungs, intestines, brain, kidneys, heart, and muscles [18], no studies have been reported on *Ch25H* expression and function in adipose tissue.

Most of the macrophages in the adipose tissue of obese or diabetic mice have been identified as activated proinflammatory M1-like macrophages. In contrast, the major macrophages in lean mice are anti-inflammatory M2-like macrophages [23]. Several studies have reported that cholesterol plays an important role in macrophage differentiation. Functional studies on SCAP have revealed that the regulation of the activity of SREBP is associated with the formation of cholesterol crystals [24], which indicates a link between macrophage differentiation and metabolic diseases. However, the role of SCAP in macrophages is not completely understood.

Here, we showed that SCAP KO macrophages link the regulation of cholesterol efflux to the acceleration of M1 polarization in ATMs, thereby increasing adipose tissue inflammation and insulin resistance. We observed that *Ch25H* gene expression was reduced in SCAP KO macrophages. Consistent with our earlier report (Im et al Cell Met. 2011), LPS-induced SREBP-1a stimulated cholesterol synthesis, but it also leads to increased 25-HC levels, via SREBP-1a dependent activation of *Ch25H* gene expression as well. Decreases in 25-HC levels resulted in reduced liver X receptor alpha (LXRα)-mediated cholesterol efflux in macrophages, suggesting that intracellular free cholesterol might accumulate due to the reduced cholesterol efflux in SCAP KO macrophages. In addition, a high-fat high- sucrose diet resulted in increased M1 macrophage infiltration in SCAP mKO mice, suggesting that SCAP may play a pivotal role in dietary regulated macrophage polarization and obesity. These results suggest that obesity was induced in SCAP mKO mice via the regulation of the SCAP-SREBP-1a pathway-stimulated activation of *Ch25H* gene expression in ATMs. Our results indicate that the activation of this pathway in macrophages may provide a novel therapeutic strategy against obesity via the regulation of cholesterol homeostasis in ATMs.

Material and methods

Animal models

The SCAP floxed allele was generated from the mixed strain originally described [8] by back-crossing onto C57BL/6J mice for

over 10 generations [12], and SCAP mKO mice were generated by crossing SCAP$^{fl/fl}$ with Lyz2-Cre mice. SREBP-1a-deficient (1aDF) and SREBP-1c KO (1cKO) mice lines were housed as described previously [12,25]. All of the backcrossed mice used in this study were further backcrossed for 3–4 more round to facilitate recombination and maintain the C57BL/6J background. C57BL/6J mice were purchased from the Jackson Laboratory (Stock #000664, Bar Harbor, ME, USA) and used as a control for 1aDF and 1cKO mice. Age-matched male SCAP mKO and SCAP$^{fl/fl}$ mice (8 weeks old) were randomly assigned to groups fed normal chow (CD) or a high-fat/high-sucrose diets (HFHS) (D12327, 40% fat and sucrose as kcal, Research Diets, NJ, USA) for 16 weeks (n = 4–7 per group). Body weight and food consumption were monitored weekly, and body composition was assessed using nuclear magnetic resonance (NMR, LF50 BCA-Analyzer, Bruker, Brussels, Belgium). All mice were housed in ventilated cages at 22–24 °C under a 12 h light-dark cycle in a specific pathogen-free facility. All animal experiments were approved by the Animal Care and Use Committees of the Keimyung University School of Medicine, Daegu, Republic of Korea (IRB #KM-2016-22R1).

Isolation of bone marrow-derived macrophages (BMDMs)

BMDMs were isolated from C57BL/6J, SCAP$^{fl/fl}$, SCAP mKO, 1aDF, and 1cKO mice as described previously [12]. Briefly, femurs and tibias were isolated and flushed with Dulbecco's modified Eagle's medium (DMEM) including 2% fetal bovine serum (Hyclone, Logan, UT, USA). After removing red blood cells by ammonium-chloride-potassium (ACK) lysis buffer (Invitrogen, Carlsbad, CA, USA), macrophages were plated and differentiated in culture with 20% L929 complement DMEM for 7 days. The BMDMs were polarized into M1 or M2 macrophages after 24 h of culturing using the indicated activators: 100 ng/ml LPS (Sigma-Aldrich, MO, USA) or 20 ng/ml recombinant mouse IL-4 (R&D System, Minneapolis, MN, USA) for M1 vs M2 polarization, respectively.

Isolation of adipose stromal vascular fractions (SVFs)

Mouse adipose tissues were isolated and digested with 0.1% collagenase type I (Worthington Biochemical Corp., Freehold, NJ, USA) for 45 min at 37 °C using the gentleMACS™ Dissociator (Miltenyi Biotech Inc. Bergisch Gladbach, Germany). The digested adipose tissues were filtered through a 70 μM cell strainer and centrifuged at 500*g* for 5 min to separate the SVFs from the adipocytes. The SVF pellets were then collected and resuspended in ACK lysis buffer to remove red blood cells prior to further analysis.

Flow cytometric analysis

SVFs and BMDMs were washed and stained with FITC-anti-integrin subunit alpha M (CD11b, 101205, BioLegend, San Diego, CA, USA), PE-Cy7-anti-F4/80 (25-4801-82, Invitrogen), APC-anti-integrin, and alpha X (CD11c, 117309, BioLegend), PE-anti-CD86 (105607, BioLegend), and PE- mannose receptor C-type 1 (CD206, 141705, BioLegend). The cells were then subjected to flow cytometric analysis using BD FACS Caliber (BD Biosciences, San Jose, CA, USA).

Intracellular cholesterol assay

A cholesterol assay was performed on BMDMs using the Cholesterol assay kit (ab133116, Abcam, Cambridge, MA, USA) that monitored intracellular filipin staining according to the manufacturer's instructions [26]. Subsequently, isolated BMDMs (5×10^5 cells/well) were seeded overnight in 8-well chamber slides (Lab-Tek II, Nalgene Nunc, Naperville, IL, USA) and cultured in control medium or media containing 100 ng/ml LPS. The images were acquired using confocal laser scanning microscopy (Carl Zeiss, Oberkochen, Germany). The fluorescent intensity of the cells with filipin staining was quantified using the ImageJ software version 1.53r (NIH, Bethesda, MD, USA). Outlines of the cells were drawn manually.

Statistical analysis

All results are presented as the mean ± SEM. All statistical analyses were performed in GraphPad Prism version 8.4.3 (GraphPad Software Inc., La Jolla, United States). Comparisons between two groups were performed using an unpaired *t*-test. Probability values $p < 0.05$ were considered statistically significant.

Results

SCAP mKO mice are more susceptible to HFHS-induced fat accumulation

To evaluate the potential contribution of macrophage-specific SCAP to metabolic diseases, we compared weight gain in SCAP$^{fl/fl}$ and SCAP mKO mice fed an HFHS diet or CD (Fig. 1). Both lines gained significant weight by 16 weeks, but the SCAP mKO mice gained significantly more weight than SCAP$^{fl/fl}$ mice (Fig. 1A). However, food consumption levels expression levels didn't differ between genotypes (Fig. S1A). And leptin gene expression was increased in eWAT of HFHS-fed mice groups, but there was no difference of leptin level between genotypes (Fig. S1B). Most of the excess weight in the HFHS-fed SCAP mKO mice was due to increased fat mass (Fig. 1B). Simultaneously, lean body mass decreased in SCAP mKO mice (Fig. 1C). Furthermore, upon visual inspection, the epididymal white adipose tissue (eWAT) depot was enlarged in HFHS-fed SCAP mKO mice (Fig. 1D) and furthermore, fat pad weights of eWAT and inguinal white adipose tissue were higher in HFHS-fed SCAP mKO than in SCAP$^{fl/fl}$ mice (Fig. 1E and F). Histologically, SCAP mKO mice had larger adipocytes in eWAT than SCAP$^{fl/fl}$ mice, reflected in the average size of the adipocytes; in addition, F4/80 staining showed that macrophage infiltration was increased in SCAP mKO mice (Fig. 1G). These results suggested that the size of adipocytes and macrophage infiltration were increased in adipose tissue of SCAP mKO mice and that SCAP deficiency in macrophages increases the severity of obesity and metabolic disease.

SCAP mKO mice have a reduced energy expenditure and induce insulin resistance

Next, we assessed energy expenditure using metabolic cages. In accordance with the increase in body weight gain and elevated body fat mass, the whole-body energy expenditure of SCAP mKO mice on HFHS diet was slightly reduced relative to control SCAP$^{fl/f}$ mice (Fig. 2A), and this was accompanied by a slight decrease in physical activity (Fig. 2B). To assess the metabolic consequences of SCAP deficiency in macrophages, we analyzed plasma cholesterol and free fatty acids levels. Total cholesterol, high-density lipoprotein-cholesterol, low-density lipoprotein-cholesterol, and non-esterified fatty acid (NEFA) levels were higher in HFHS-fed SCAP mKO than in SCAP$^{fl/fl}$ mice (Fig. S1C-F). In addition, there was a significant increase in plasma aspartate aminotransferase and alanine aminotransferase levels, indicating more liver damage in SCAP mKO mice (Fig. S1G and H).

To evaluate nutrient metabolism, we performed glucose tolerance and insulin tolerance tests in HFHS-fed mice. Compared to SCAP$^{fl/fl}$ mice, SCAP mKO mice showed impaired glucose tolerance (Fig. 2C). However, glucose tolerance did not differ between the

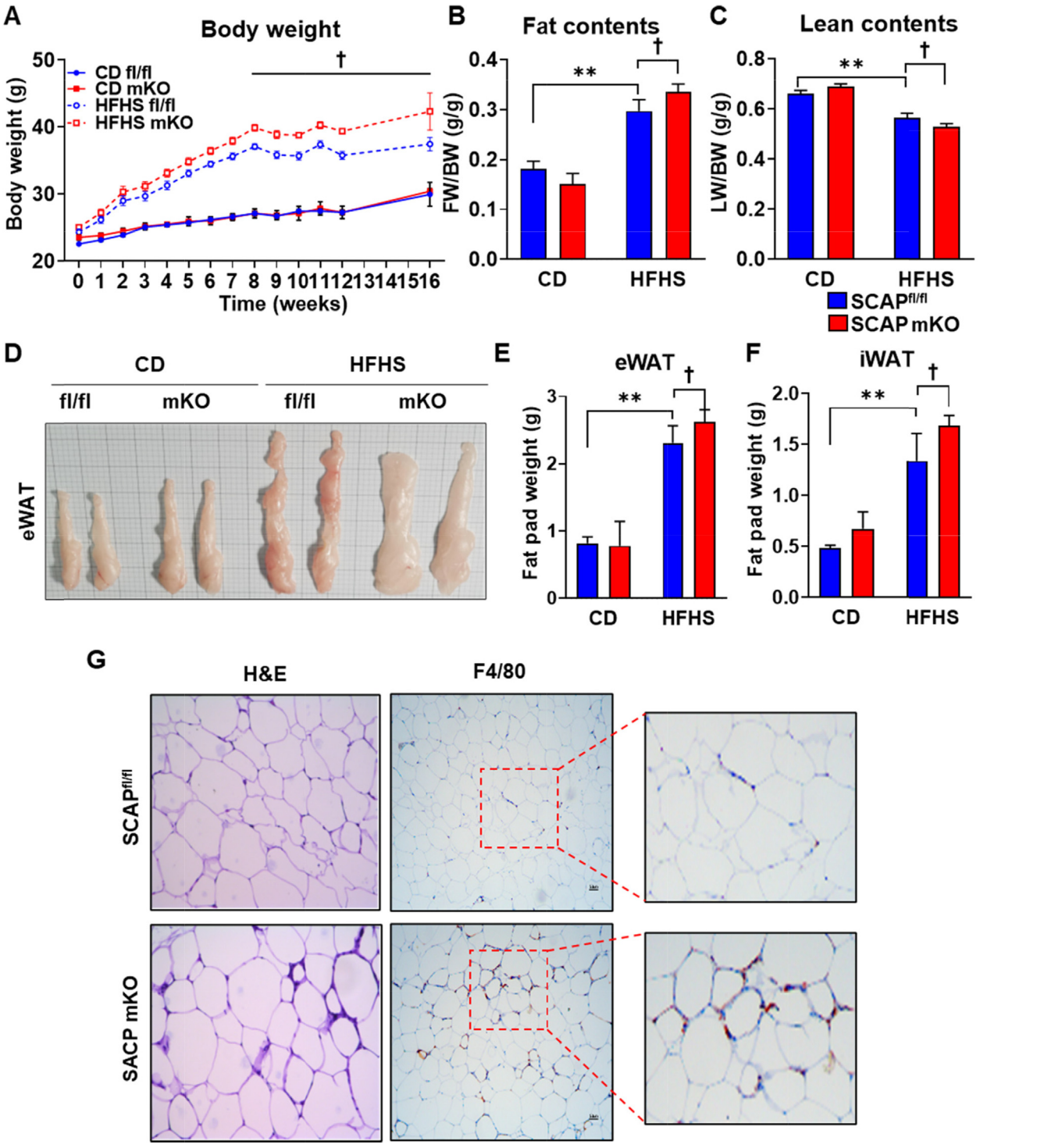

Fig. 1. Macrophage SCAP ablation increased body weight and fat mass. (A) Body weight of SCAP$^{fl/fl}$ and SCAP mKO mice fed normal chow diet (CD) or high-fat high-sucrose (HFHS) diets for 16 weeks (n = 6 per each group). (B and C) Fat and lean body mass were normalized by body weight. (D) Representative images of epididymal white adipose tissue (eWAT) from CD or HFHS diet-fed SCAP$^{fl/fl}$ and SCAP mKO mice. SCAP$^{fl/fl}$ and SCAP mKO mice (n = 6 per group) were fed either CD or HFHS diets for 16 weeks. (E) The weight of eWAT. (F) The weight of inguinal white adipose tissue (iWAT). (G) Hematoxylin and eosin (H&E) staining or immunohistochemistry using anti-F4/80 on eWAT sections (5 μm) of SCAP$^{fl/fl}$ and SCAP mKO mice exposed to HFHS diets for 16 weeks. The regions within the squares are enlarged on the right. Values are expressed as mean ± SEM. $^{**}p < 0.01$ compared to CD-fed SCAP$^{fl/fl}$ mice. $^{\dagger}p < 0.05$ compared to HFHS-fed SCAP$^{fl/fl}$ mice.

CD-fed groups for both genotypes. These results were confirmed by measuring the area under the curve (AUC) values (Fig. 2D). SCAP mKO mice showed mildly impaired insulin sensitivity (Fig. 2E and F). Additionally, serum insulin levels in SCAP mKO mice were higher than in WT mice (Fig. S1I). But there were no differences in serum glucose levels between genotypes (Fig. S1J). Homeostasis model assessment of insulin resistance (HOMA-IR) analysis confirmed that there was an increase in insulin resistance in HFHS-fed SCAP mKO mice (Fig. S1K). These results indicated that SCAP mKO mice were more susceptible to increases in metabolic dysfunction owing to increases in fat accumulation after the consumption of HFHS diet.

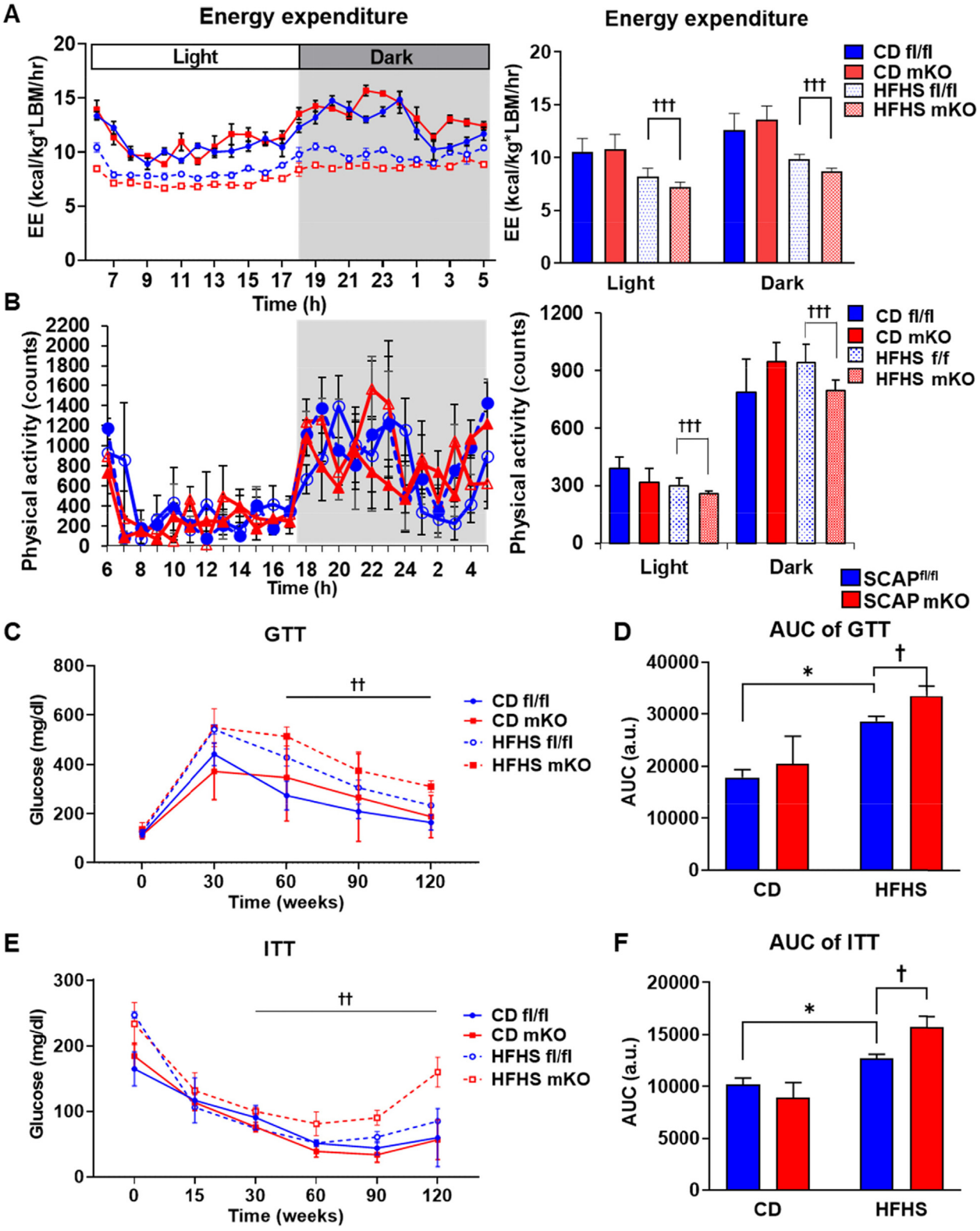

Fig. 2. Macrophage SCAP deletion promoted diet-induced insulin resistance. (A) Energy expenditure (EE) over 24 h period using metabolic cages. $SCAP^{fl/fl}$ and SCAP mKO mice fed CD or HFHS diet. Average EE over the light and dark phases (right panel). (B) Metabolic cage studies were performed in a CD or a HFHS diet fed $SCAP^{fl/fl}$ or SCAP mKO mice. The physical activity and average physical activity during indicated period (right panel). (C) Glucose tolerance test (GTT) of $SCAP^{fl/fl}$ and SCAP mKO mice after 16 weeks on CD or HFHS diet. (D) Quantification of GTT area under the curve (AUC). (E) Insulin tolerance test (ITT) of $SCAP^{fl/fl}$ and SCAP mKO mice after 16 weeks on CD or HFHS diets. (F) Quantification of ITT AUC. Values are expressed as mean ± SEM. $^{*}p < 0.05$ compared to CD-fed $SCAP^{fl/fl}$ mice. $^{\dagger}p < 0.05$, $^{\dagger\dagger}p < 0.01$ and $^{\dagger\dagger\dagger}p < 0.001$ compared to HFHS-fed $SCAP^{fl/fl}$ mice.

Numbers of M1 macrophages are increased in the adipose tissue of HFHS-fed SCAP mKO mice

To evaluate macrophage accumulation and polarization in adipose tissue, the expression of M1 and M2 ATM marker genes was assessed in eWAT of HFHS-fed mice. The expression levels of macrophage infiltration and M1 marker genes encoding F4/80, monocyte chemoattractant protein 1 (MCP1), CD11c were increased (Fig. 3A), whereas those of M2 maker genes encoding IL-10, CD206, c-type lectin domain containing 10a (Clec10a), and inflammatory zone 1 (Fizz1) were significantly downregulated in eWAT of HFHS-fed SCAP mKO mice (Fig. 3B). These results suggested that SCAP macrophage-specific deficiency increases M1 macrophage polarization and macrophage infiltration in eWAT, which could accelerate fat accumulation. We further quantified ATMs in eWAT from HFHS-fed SCAP$^{fl/fl}$ and SCAP mKO mice using

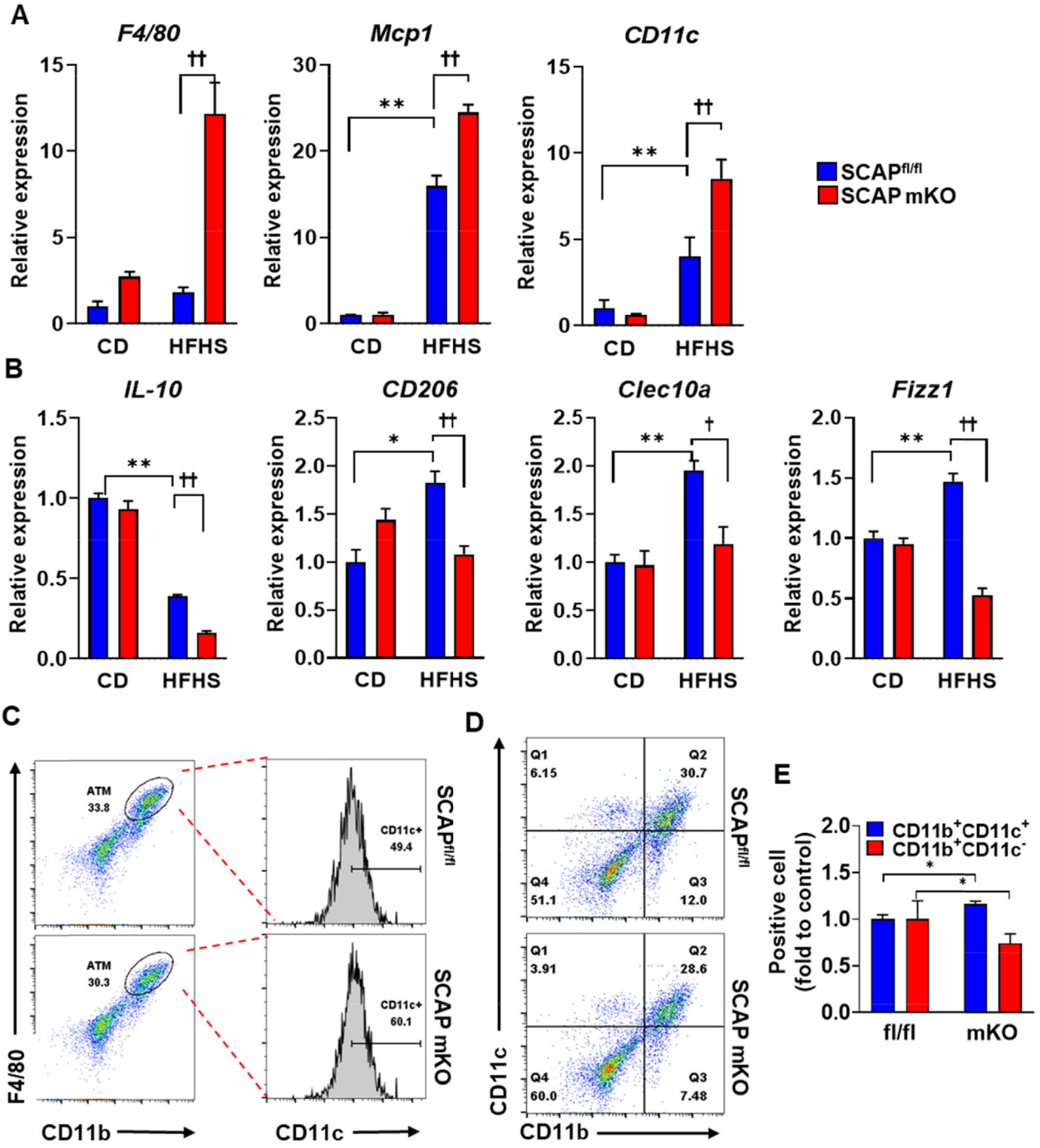

Fig. 3. SCAP deficiency in macrophages increased M1 polarization in eWAT of HFHS diet-fed SCAP mKO mice. SCAP$^{fl/fl}$ and SCAP mKO mice (n = 6 per each group) were fed either CD or HFHS diet for 16 weeks. (A) mRNA levels of M1 macrophage markers, *F4/80*, *Mcp1*, and *CD11c* in eWAT. (B) Gene expression levels of M2 macrophage markers, such as *IL-10*, *CD206*, *Clec10a*, and *Fizz1* in the eWAT were assessed using qPCR. The Ct values obtained were normalized to that of L32. (C) SCAP$^{fl/fl}$ and SCAP mKO mice were fed either CD or HFHS diet for 16 weeks. The macrophage composition of the SVFs prepared from eWAT was analyzed using FACS. Flow cytometric analysis of CD11c population in CD11b$^+$ F4/80$^+$ cells among SVF cells of eWAT. (D) Representative flow cytometry histograms showing CD11b and CD11c population in SVF cells of eWAT. (E) Quantitative analyses of M1 (CD11b$^+$CD11c$^+$) and M2 macrophages (CD11b$^+$ CD11c$^-$). Values are expressed as mean ± SEM. $^*p < 0.05$ and $^{**}p < 0.01$ compared to CD-fed SCAP$^{fl/fl}$ mice. $^{\dagger}p < 0.05$ and $^{\dagger\dagger}p < 0.01$ compared to HFHS-fed SCAP$^{fl/fl}$ mice. SVF: stromal vascular fractions.

flow cytometry to confirm the gene expression data. The SVFs isolated from eWAT of SCAP$^{fl/fl}$ and SCAP mKO mice were stained for CD11b^{+} and F4/80, which are M1 macrophage markers. The population of CD11b^{+}-stained macrophages in SCAP mKO mice was higher than that in SCAP$^{fl/fl}$ mice, indicating that the M1 ATM population was increased in SCAP mKO mice (Fig. 3C). Next, BMDMs were stained for CD11c^{+} as a marker of M2 macrophages, and M2 macrophages in eWAT were counted. Consistent with the gene expression profiles, the number of M2 macrophages was lower in eWAT of SCAP mKO mice (Fig. 3D). These results demonstrated that M1 ATMs were significantly enriched in SCAP mKO mice, whereas the number of M2 macrophages was reduced in the eWAT of SCAP mKO mice.

M1 macrophage polarization is increased in SCAP KO macrophages

Previous studies have demonstrated that the function of SREBPs contribute to innate immune responses in macrophages [11]. To eveluate the function of SCAP in macrophage polarization, we isolated BMDMs from SCAP$^{fl/fl}$ and SCAP mKO mice and induced macrophage polarization to M1 and M2 by treating them with LPS (100 ng/ml) or IL-4 (20 ng/ml), respectively. The LPS dependent increase in expression of genes related to proinflammatory cytokine secretion, such as IL-12 subunit beta (*IL-12β*), *IL-6,* and *IL-1β,* was significantly higher in SCAP KO macrophages (Fig. 4A). To assess the effects on IL-1β secretion, the BMDMs were exposed to LPS and treated with adenosine triphosphate (ATP). IL-1β secretion was also higher in SCAP KO BMDMs than in SCAP$^{fl/fl}$ BMDMs (Fig. 4B). In contrast, M2 polarization markers including *Fizz1*, arginase 1 (*Arg1*), *CD206*, *IL-10,* and *Clec10a* were reduced following IL-4 treatment in SCAP KO BMDMs (Fig. 4C). Next, macrophage M1/M2 polarization was evaluated using gene expression and flow cytometric assays. The FACS analysis showed that M1 polarization of macrophages in SCAP KO BMDMs was increased after LPS treatment as analyzed by staining for F4/80 and CD86 (Fig. 4D and E), whereas the IL-4 treatment showed decreased M2 polarization which was assessed by staining for F480 and CD206 (Fig. 4F and G). These results suggest that SCAP deficiency in macrophages increases M1 polarization while impairing M2 polarization.

SCAP transcriptionally induces Ch25H gene expression via regulation of SREBP-1a

SCAP mRNA levels were reduced by approximately 80% in SCAP KO BMDMs (Fig. 5A). The RNA expression for the three SREBP isoforms was assessed using quantitative polymerase chain reaction (qPCR) (Fig. 5B) and protein levels for SREBP-1 were measured by western blotting (Fig. 5C). The results showed that the expression of *Srebp-1c* and *Srebp-2*, but not that of *Srebp-1a,* were downregulated in SCAP KO macrophages (Fig. 5B and C). This is likely because SREBP-1c and -2 genes are auto-regulated by SREBPs. LPS induced the expression of nuclear SREBP-1 protein in SCAP$^{fl/fl}$ BMDMs as observed in our earlier report [27], but not in SCAP KO macrophages (Fig. 5C). The expression of lipogenic genes, such as those encoding fatty acid synthase, acetyl-CoA carboxylase 1, 3-hydroxy-3-methyl-glutaryl-CoA reductase, and stearoyl-CoA desaturase-1, did not differ between the genotypes (Fig. 5D).

Regulation of cholesterol efflux is of particular importance to macrophage lipid homeostasis during innate immune responses [28], so we measured ABCA1 and ABCG1 expression in BMDMs from SCAP$^{fl/fl}$ and SCAP mKO mice. ABCA1 and ABCG1 mRNA (Fig. 5E) and protein (Fig. 5F) levels were significantly reduced in SCAP KO macrophages. Interestingly, *Abca1* and *Abcg1* expression levels were restored in SCAP KO BMDMs by ectopic expression of SREBP-1a from an adenovirus vector (ad-SR-1a) (Fig. 5G and H). Furthermore, *Abca1* and *Abcg1* expression were also lower in 1aDF BMDMs which only lack the SREBP-1a isoform (30), and once again, expression was recovered by supplying SREBP-1a ectopically (Fig. 5I and J).

SCAP regulates cholesterol efflux via SREBP-1a-mediated Ch25h

ABCA1 and ABCG1 expression are known to be directly regulated by the oxysterol activated LXR and a major macrophage endogenous macrophage selective oxysterol is 25-HC which is produced from cholesterol through the action of ch25 hydroxylase. Interestingly, LXR induced proinflammatory responses via the regulation of macrophage *Ch25H* expression [22] and another study demonstrated that cholesterol synthesis was regulated by LPS in macrophages [29]. To investigate the role of *Ch25H* in our studies, we treated BMDMs with LPS and assessed whether *Ch25H* mRNA expression was affected (Fig. 6A). Consistent with previous results, *Ch25H* expression was stimulated by LPS in SCAP$^{fl/fl}$ BMDMs, however this was significantly blunted in SCAP KO BMDMs, suggesting that *Ch25H* transcription might be dependent on SREBPs. We ectopically expressed the individual human SREBP-1a, SREBP-1c, or SREBP-2 from adenovirus vectors in SCAP$^{fl/fl}$ and SCAP KO BMDMs and interestingly, *Ch25H* expression was more sensitive to activation by *SREBP-1a* overexpression in SCAP KO BMDMs, although SREBP-1c and SREBP-2 both induced *Ch25H* gene expression to lower levels (Fig. 6B).

In an earlier study, we found that LPS stimulated SREBP-1 mRNA and protein production in BMDMs [27] and we showed that SREBP-1a mRNA is ten-fold higher than SREBP-1c. To evaluate which SREBP-1 isoform might be involved in stimulation of *Ch25H* expression we measured Ch25H expression in BMDM derived from mice that were specifically lacking either SREBP-1a (1aDF) or SREBP-1c (1cKO). The data in Fig. 6C shows LPS-stimulated *Ch25H* mRNA was reduced in 1aDF but not in SREBP-1cKO BMDM. Next, we measured intracellular cholesterol levels in LPS-treated BMDMs using filipin staining as the read out. First, we found that BMDMs of SCAP mKO mice exhibited an increased filipin fluorescent intensity after LPS stimulation (Fig. 6D). There was also an increase in filipin intensity in BMDMs from 1aDF mice (Fig. 6E). Collectively, these data are consistent with a significant role for SCAP and SREBP-1a in regulating intracellular cholesterol levels by balancing synthesis and efflux.

Because Ch25H expression was reduced in SREBP-1aDF BMDM we investigated whether it might be a direct transcriptional target of SREBP-1. First, we identified three highly conserved potential SREBP response elements (SRE) in the mouse *Ch25H* gene promoter (Fig. 6F) and assessed promoter activity and SREBP transactivation through a transient transfection assay protocol in human embryonic kidney 293 T (HEK 293 T) cells. The mouse *Ch25H* gene promoter was activated by the overexpression of SREBP-1a (Fig. 6G). The binding of SREBP-1 to these SREs were then evaluated at the chromatin level using a chromatin immunoprecipitation assay with an antibody to SREBP-1 and BMDM chromatin from WT and 1aDF mice. The data show SREBP binds specifically to sites labeled 1 and 2 of the mouse *Ch25H* gene promoter (Fig. 6H and I). Taken together, the expression data in the mutant macrophages and the direct activation and ChIP studies suggest that *Ch25H* is likely a putative direct target of SREBP-1a in macrophages and that SREBP-1a might act as a key mediator of the SCAP-Ch25H regulatory axis.

To determine whether this mechanism revealed in detailed studies in BMDM might help explain the weight gain and metabolic disease phenotypes in the SCAP mKO mice, we first evaluated gene expression levels for *Srebp-1a*, *Ch25H*, *Abca1,* and *Abcg1* in the ATMs of eWAT from HFHS-fed SCAP$^{fl/fl}$ and SCAP mKO mice. Consistent with previous results, the gene expression levels of *Ch25H*, *Srebp-1a,* and *Abca1* were significantly lower in SCAP

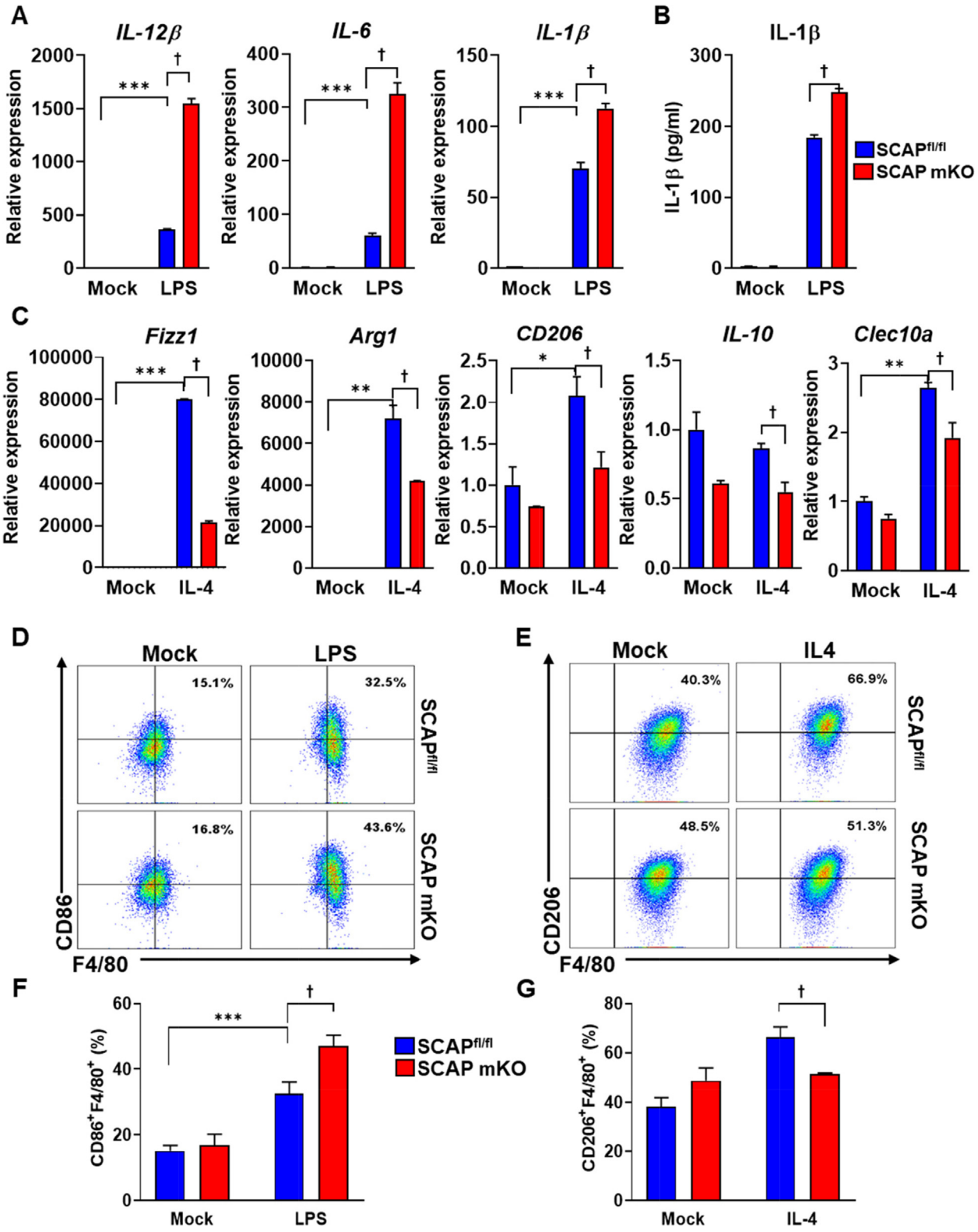

Fig. 4. Abrogation of SCAP increased M1 but decreased M2 polarization of macrophages. (A) Relative mRNA expression levels of M1 macrophage marker genes. BMDMs from SCAP$^{fl/fl}$ and SCAP mKO mice (n = 3 per group) were treated with 100 ng/ml LPS for 24 h. qPCR was used for analyzing *IL-12β*, *IL-6*, and *IL-1β* mRNA expression. (B) IL-1β secretion level in BMDMs of SCAP$^{fl/fl}$ and SCAP mKO mice. BMDM were treated with LPS for 6 h, followed by incubation with 1 mM ATP for 30 min. IL-1β secretion levels were measured using ELISA. (C) Relative mRNA expression levels of M2 macrophage marker genes. BMDMs were treated with 20 ng/ml IL-4 for 24 h. qPCR was used for analyzing *Fizz1*, *Arg1*, *CD206*, *IL-10*, and *Clec10a* mRNA expression. (D) Flow cytometric analysis of BMDMs after incubation with LPS (100 ng/ml). SCAP$^{fl/fl}$ and SCAP KO BMDMs (n = 3 per group) were treated with 100 ng/ml LPS for 24 h. Flow cytometric analysis of F4/80 and CD86 population. (E) Flow cytometric analysis data for M2 polarization. BMDMs were treated with 20 ng/mL IL-4 for 24 h. Flow cytometric analysis of F4/80 and CD206 population. (F) The percentage of F4/80$^+$CD86$^+$ cells. (G) The percentage of F4/80$^+$CD206$^+$ cells. Values are expressed as mean ± SEM. Representative results from three repeated experiments are shown. $^*p < 0.05$, $^{**}p < 0.01$ and $^{***}p < 0.001$ compared to Mock SCAP$^{fl/fl}$ mice. $^{\dagger}p < 0.05$ compared to LPS- or IL-4-treated SCAP$^{fl/fl}$ mice.

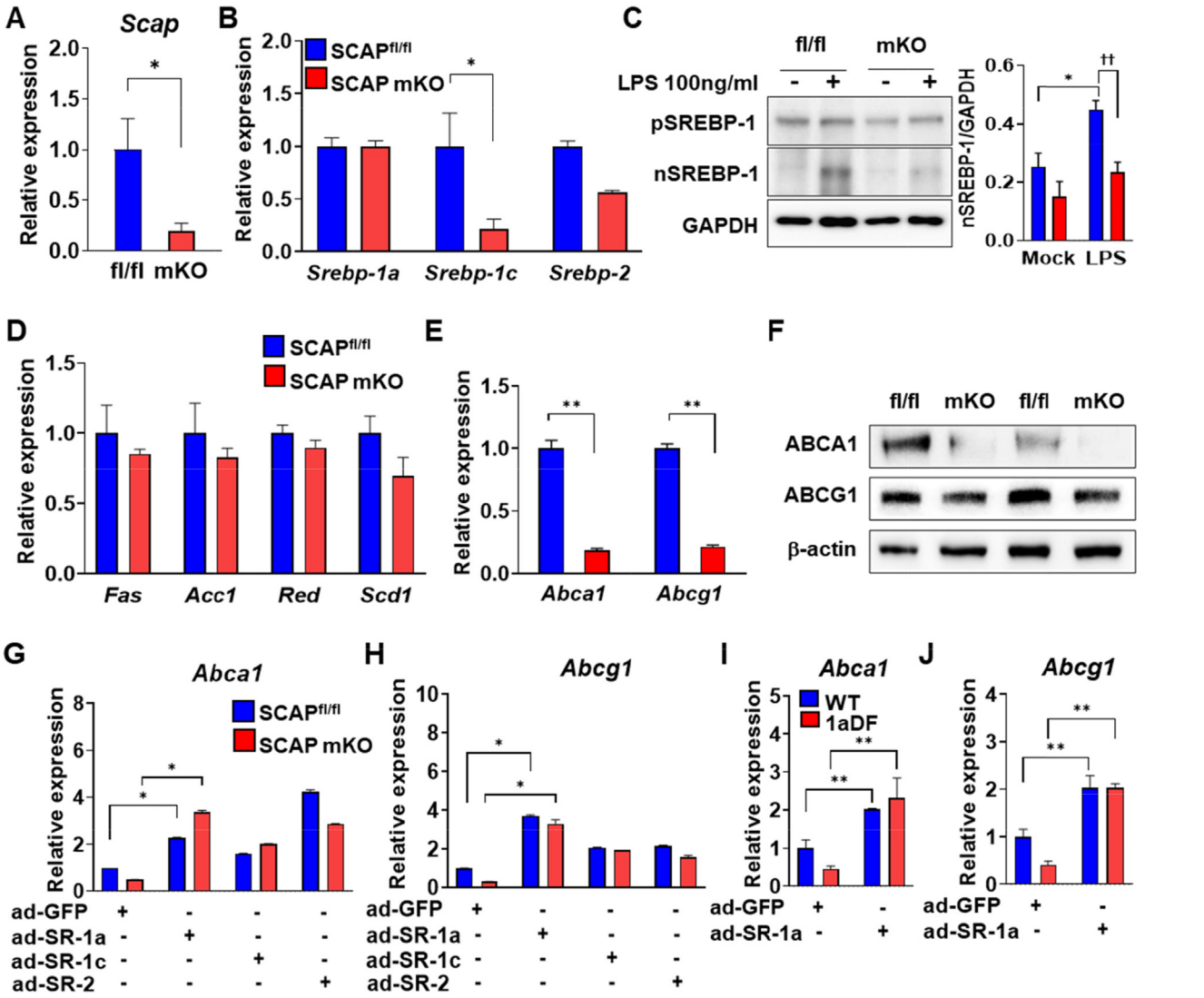

Fig. 5. SCAP regulates the expression of cholesterol efflux-related genes via regulation of SREBP-1a. (A) qPCR analysis of *Scap* mRNA expression in SCAP$^{fl/fl}$ and SCAP KO BMDMs (n = 3 per group). Results were normalized to L32 mRNA and relative *Scap* mRNA levels are presented. (B) qPCR analysis of *Srebp-1a*, *−1c*, and *−2* mRNA expression in BMDMs. (C) Precursor and mature forms of SREBP-1 in LPS-treated BMDMs. BMDMs were incubated with medium or LPS (100 ng/ml) for 24 h. Protein levels of nuclear SREBP-1 were analyzed using immunoblotting (left panel), quantified using ImageJ software, and normalized using GAPDH levels (right panel). (D) mRNA levels of SREBP target genes such as *Fas*, *Acc1*, *Red*, and *Scd1* were measured using qPCR. (E) mRNA expression levels of *Abca1* and *Abcg1*. mRNA levels of *Abca1* and *Abcg1* in SCAP$^{fl/fl}$ and SCAP KO BMDMs were determined using qPCR. (F) Immunoblot analysis for determining ABCA1 and ABCG1 protein levels. Protein samples were prepared from SCAP$^{fl/fl}$ and SCAP KO BMDMs. (G and H) mRNA expression in BMDMs of SCAP$^{fl/fl}$ and SCAP mKO mice (n = 6 each group) infected with adenoviruses for GFP (ad-GFP), SREBP-1a (ad-SR-1a), SREBP-1c (ad-SR-1c), and SREBP-2 (ad-SR-2). qPCR analysis for *Abca1 A* and *Abcg1 B* expression. (I and J) mRNA expression of *Abca1* and *Abcg1*. BMDMs of WT and 1aDF mice were infected with ad-GFP or ad-SR-1a for 72 h. $^{*}p < 0.05$ and $^{**}p < 0.01$ compared to Mock SCAP$^{fl/fl}$ mice and ad-GFP group. $^{\dagger\dagger}p < 0.01$ compared to LPS-treated SCAP$^{fl/fl}$ mice. (For interpretation of the references to colour in this figure legend, the reader is referred to the web version of this article.)

mKO ATMs, although Abcg1 mRNA levels was only slightly decreased (Fig. 7A-D). These results confirmed that SCAP-Ch25H regulatory axis we described in BMDM likely plays a significant role in the response of ATMs to HFHS challenge.

Discussion

In this study, we showed that SCAP deletion exacerbated HFHS-induced polarized proinflammatory macrophage infiltration in adipose tissue, which might significantly stimulate the secretion of proinflammatory cytokines and induce metabolic diseases such as obesity and diabetes (Fig. 7E).

A recent study reported that cholesterol recycling was impaired in M1-like macrophages of adipose tissue in individuals with obesity [30]. Therefore, increases in the number of M1-like macrophages in SCAP mKO mice might aggravate HFHS-mediated fat accumulation and dysregulation of cholesterol efflux in adipose tissue. Furthermore, previous study on SCAP have revealed a mechanism of inhibition of fatty liver formation using liver-specific SCAP KO mice [31]. In SCAP mKO mice, fat accumulation and fatty liver formation were expected to decrease; however, we observed that fat accumulation increased in both livers and adipose tissue from SCAP mKO mice on an HFHS diet (Fig S2). Although expression levels of lipogenic genes were lower in the livers of SCAP mKO mice (Fig. S3A and B), hepatic steatosis might be associated with increased transcription of genes involved in liver fibrosis, macrophage infiltration, and proinflammation (Fig. S3C-F). Presumably, it appears that most macrophages infiltrating the adipose tissue differentiated into the M1 population. Several factors, granulocyte-macrophage-colony stimulating factor, interferon gamma (IFN-γ), and LPS, are involved in the differentiation into

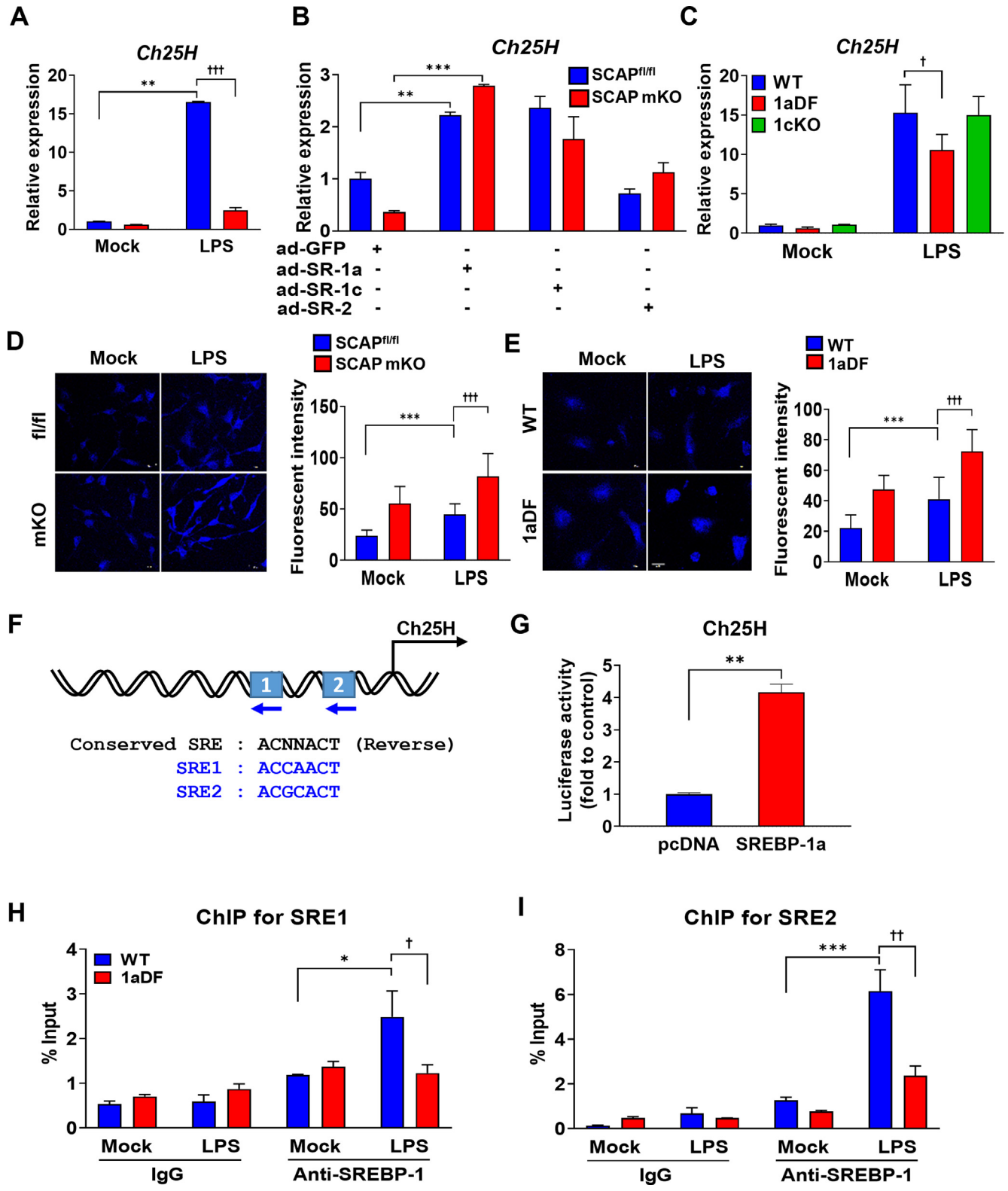

Fig. 6. *Ch25H* is the putative target of SREBP in SCAP mKO. (A) *Ch25H* gene expression levels in BMDMs. BMDM were incubated with 100 ng/ml LPS for 24 h. (B) The expression levels of the *Ch25H* gene by overexpression of SREBP isoforms in BMDMs. *Ch25H* mRNA expression was assessed using qPCR in the BMDMs infected with adenoviruses harboring ad-GFP, ad-SR-1a, ad-SR-1c, and ad-SR-2. (C) mRNA level of *Ch25H* in LPS-treated BMDMs extracted from WT, 1aDF, and 1cKO mice. (D) Representative filipin staining of $SCAP^{fl/fl}$ and SCAP KO BMDMs (left). Quantification of the filipin staining intensity (right). (E) Filipin expression in BMDMs from WT and 1aDF mice (left). Quantification of filipin immunofluorescence intensity in BMDMs (right). BMDMs were incubated with 100 ng/ml LPS for 24 h. (F) The putative SREBP-1 response element (SRE) on mouse *Ch25H* gene promoter. The locations of the three highly conserved SREs from the transcription start site are indicated. (G) *Ch25H* promoter activity. Plasmid constructs of mouse *Ch25H* gene promoter was transiently transfected into HEK 293 T cells, and the luciferase assay was performed. (H and I) ChIP assay for SREBP-1 binding on chromatin from $SCAP^{fl/fl}$ and SCAP KO BMDMs. Chromatin from BMDMs was analyzed for recruitment of SREBP-1 to the SRE region of mouse *Ch25H* promoter using ChIP assay. Values are expressed as mean ± SEM. $^{*}p < 0.05$, $^{**}p < 0.01$, and $^{***}p < 0.001$ compared to Mock WT or $SCAP^{fl/fl}$ mice, ad-GFP group, or pcDNA group. $^{\dagger}p < 0.05$, $^{\dagger\dagger}p < 0.01$, and $^{\dagger\dagger\dagger}p < 0.001$ compared to LPS-treated WT or $SCAP^{fl/fl}$ mice.

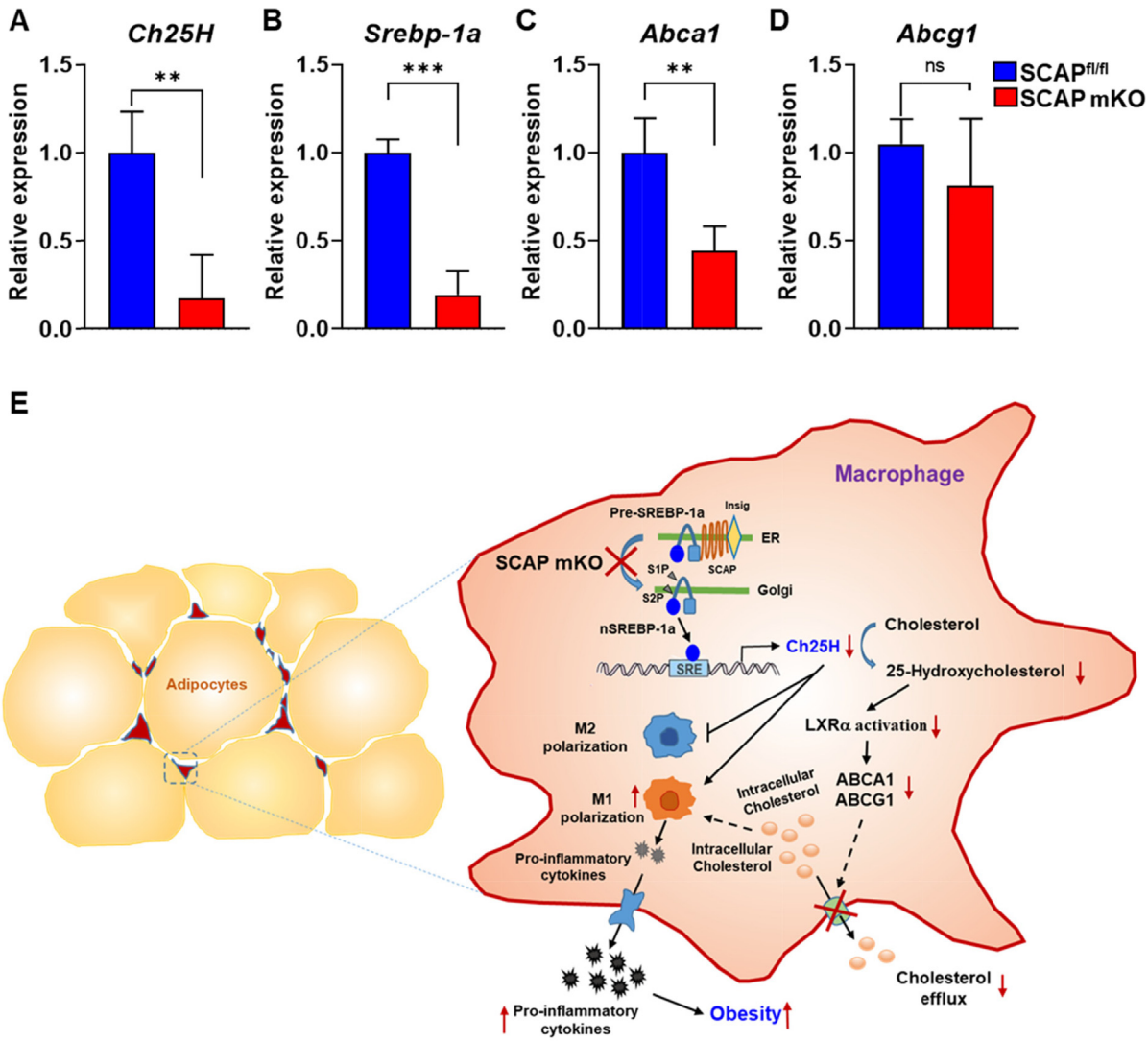

Fig. 7. Deficiency of SCAP regulation in macrophages reduces intracellular cholesterol content via suppression of *Ch25H* gene expression in eWAT. SCAP$^{fl/fl}$ and SCAP mKO mice (n = 5 per group) were fed HFHS diets for 16 weeks. (A-D) Relative mRNA expression levels of *Ch25H, Srebp-1a, Abca1,* and *Abcg1*. The macrophage gene expression of the SVFs isolated from eWAT was analyzed using qPCR. (E) Proposed mechanism for SCAP in macrophage polarization of adipose tissue in metabolic diseases. Values are expressed as mean ± SEM. $^{**}p < 0.01$ and $^{***}p < 0.001$ compared to SCAP$^{fl/fl}$ mice.

M1 macrophages [32,33]. However, studies on the mechanism of M1 differentiation by SCAP are lacking. Here, we suggested that M1 macrophage polarization might be regulated by SCAP.

IFN-γ is a major activator of the innate and adaptive immune responses [34,35]. Studies also show that Ch25H is directly activated by STAT1 signaling downstream from INF. In this study, IFN-γ activated Ch25H and SREBP-1a genes expression in BMDMs from SCAP$^{fl/fl}$ and WT mice, but not SCAP mKO and 1aDF BMDMs (Fig. S4A-C). In addition, IFN-γ-treated BMDMs resulted in an increase the accumulation of SREBP-1 protein as well (Fig. S4D and E). The mechanism for how INF-γ activates SREBP-1 and whether SREBP-1 and STAT-1 synergize to activate Ch25H and 25-OH cholesterol production is an interesting direction for future investigation.

In SCAP mKO mice, we observed an increase in classical M1 macrophage infiltration in the adipose tissue. This was due to a reduction in 25-HC synthesis owing to a decrease in *Ch25H* gene expression; the expression of *Abca1* and *Abcg1* were also downregulated because the reduction in 25-HC levels which would limit their activation by LXR. In addition to activating cholesterol efflux, LXR represses proinflammatory cytokine secretion in macrophages by suppressing the expression of inflammatory genes induced by LPS or TNF-α via NF-κB signaling [36]. In several cohort studies on human obesity and insulin resistance, LXRα and LXRβ signaling was dysregulated, indicating that the reduction of LXR activity and mutant LXRs were associated with adipose tissue dysfunction and obesity [37,38]. Previous studies on mice harboring individual or double KO of LXRα and LXRβ in adipose tissue have revealed that the double KO mice showed glucose tolerance and insulin sensitivity [39]. In addition, double KO mice are resistant to diet-induced obesit [40]. These phenotypes may rely on the inhibition of adipogenesis and increased utilization of TG via lipid oxidation and adipose lipolysis. However, the results obtained with macrophages deficient in LXRs contradicted those obtained with LXR KO in adipose tissues and muscle. Although the phenotype of liver-specific SCAP KO mice was opposite to that of SCAP mKO mice, our data indicated that the phenotype of the SCAP mKO mice was similar to that of LXR-deficient macrophages. These results suggested that tissue-specific roles for LXR and SREBPs significantly contribute to development of metabolic syndrome.

In a recent study on IL-4 activated SREBP-1 regulation, M2-like macrophage activation and lipogenesis were decreased in the

BMDMs of SCAP KO mice treated with IL-4, compared with those in WT mice [41]. Similarly, we found reduced gene expression levels of the lipogenic genes and *Ch25H* in the IL-4-treated BMDMs from $SCAP^{fl/fl}$ and SCAP mKO mice. These results suggest that M2 differentiation might be controlled by SCAP and further studies will be required to evaluate the mechanism.

Conclusions

Our findings demonstrated that SCAP deficiency in macrophages accelerates the development of obesity and insulin resistance in response to HFHS diets via the regulation of *Ch25H* expression and suggested that SCAP is a key regulator of inflammatory macrophage polarization as well as cholesterol efflux and synthesis. The suppression of SCAP activity induced polarization of macrophages toward a proinflammatory phenotype and promoted fat accumulation. Indeed, the function of SCAP in macrophage polarization is systemically important, and the regulation of SREBP activity by SCAP is associated with diet-induced obesity and diabetes. As SCAP deficiency modulates macrophage polarization toward a proinflammatory phenotype in response to LPS or IL-4 treatment, these findings highlight the function of SCAP in regulating the balance in macrophage polarization and thereby preventing chronic metabolic diseases, such as obesity and insulin resistance. Hence, we revealed a mechanism by which SCAP regulates macrophage polarization, which may provide the foundation for novel therapeutic avenues for obesity and insulin resistance in the future.

Compliance with Ethics Requirements.

All experiments involving animals were conducted according to the ethical policies and procedures approved by the Institutional Animal Care and Use Committee (IACUC) in Keimyung University School of Medicine (Approval No. KM-2016-22R1).

CRediT authorship contribution statement

Jae-Ho Lee: Conceptualization, Formal analysis, Writing – original draft. **Sun Hee Lee:** Conceptualization, Formal analysis, Writing – original draft. **Eun-Ho Lee:** Resources, Writing – review & editing. **Jeong-Yong Cho:** Resources, Writing – review & editing. **Dae-Kyu Song:** Resources, Writing – review & editing. **Young Jae Lee:** Resources, Writing – review & editing. **Taeg Kyu Kwon:** Resources, Writing – review & editing. **Byung-Chul Oh:** Resources, Writing – review & editing. **Kae Won Cho:** Resources, Writing – review & editing. **Timothy F. Osborne:** Resources, Writing – review & editing. **Tae-Il Jeon:** Resources, Writing – review & editing. **Seung-Soon Im:** Conceptualization, Methodology, Software, Writing – original draft.

Declaration of Competing Interest

The authors declare that they have no known competing financial interests or personal relationships that could have appeared to influence the work reported in this paper.

Acknowledgements

This study was supported by grants of the Korea Health Technology R&D Project through the Korea Health Industry Development Institute (KHIDI), funded by the Ministry of Health & Welfare, Republic of Korea (HI14C1324) and the Korea Research Foundation and the NRF grant funded by the Korea Government (MSIP) (NRF-2021R1A4A1029238) and KMPC (2013M3A9D 5072550).

Appendix A. Supplementary material

Supplementary data to this article can be found online at https://doi.org/10.1016/j.jare.2022.05.013.

References

[1] Hill AA, Reid Bolus W, Hasty AH. A decade of progress in adipose tissue macrophage biology. Immunol Rev 2014;262(1):134–52. doi: https://doi.org/10.1111/imr.12216.
[2] Lumeng CN, Saltiel AR. Inflammatory links between obesity and metabolic disease. J Clin Invest 2011;121(6):2111–7. doi: https://doi.org/10.1172/JCI57132.
[3] Murray PJ, Wynn TA. Protective and pathogenic functions of macrophage subsets. Nat Rev Immunol 2011;11(11):723–37. doi: https://doi.org/10.1038/nri3073.
[4] Mantovani, A, Sica, A, Locati M. Macrophage polarization comes of age. Immunity 2005;23(4):344–6. doi: https://doi.org/10.1016/j.immuni.2005.10.001.
[5] Martinez FO, Sica A, Mantovani A, Locati M. Macrophage activation and polarization. Front Biosci 2008;13:453–61. doi: https://doi.org/10.2741/2692.
[6] Fujisaka S, Usui I, Bukhari A, Ikutani M, Oya T, Kanatani Y, et al. Regulatory mechanisms for adipose tissue M1 and M2 macrophages in diet-induced obese mice. Diabetes 2009;58(11):2574–82. doi: https://doi.org/10.2337/db08-1475.
[7] Wentworth JM, Naselli G, Brown WA, Doyle L, Phipson B, Smyth GK, et al. Pro-inflammatory CD11c+CD206+ adipose tissue macrophages are associated with insulin resistance in human obesity. Diabetes 2010;59(7):1648–56. doi: https://doi.org/10.2337/db09-0287.
[8] Matsuda M, Korn BS, Hammer RE, Moon YA, Komuro R, Horton JD, et al. SREBP cleavage-activating protein (SCAP) is required for increased lipid synthesis in liver induced by cholesterol deprivation and insulin elevation. Genes Dev 2001;15(10):1206–16. doi: https://doi.org/10.1101/gad.891301.
[9] Engelking LJ, Cantoria MJ, Xu Y, Liang G. Developmental and extrahepatic physiological functions of SREBP pathway genes in mice. Semin Cell Dev Biol 2018;81:98–109. doi: https://doi.org/10.1016/j.semcdb.2017.07.011.
[10] York A, Williams K, Argus J, Zhou Q, Brar G, Vergnes L, et al. Limiting Cholesterol Biosynthetic Flux Spontaneously Engages Type I IFN Signaling. Cell 2015;163(7):1716–29. doi: https://doi.org/10.1016/j.cell.2015.11.045.
[11] Oishi Y, Spann NJ, Link VM, Muse ED, Strid T, Edillor C, et al. SREBP1 Contributes to Resolution of Pro-inflammatory TLR4 Signaling by Reprogramming Fatty Acid Metabolism. Cell Metab 2017;25(2):412–27. doi: https://doi.org/10.1016/j.cmet.2016.11.009.
[12] Lee JH, Phelan P, Shin M, Oh BC, Han X, Im SS, et al. SREBP-1a-stimulated lipid synthesis is required for macrophage phagocytosis downstream of TLR4-directed mTORC1. Proc Natl Acad Sci USA 2018;115:E12228–34. doi: https://doi.org/10.1073/pnas.1813458115.
[13] Duewell P, Kono H, Rayner KJ, Sirois CM, Vladimer G, Bauernfeind FG, et al. NLRP3 inflammasomes are required for atherogenesis and activated by cholesterol crystals. Nature 2010;464(7293):1357–61. doi: https://doi.org/10.1038/nature08938.
[14] Rajamäki K, Lappalainen J, Öörni K, Välimäki E, Matikainen S, Kovanen PT, et al. Cholesterol crystals activate the NLRP3 inflammasome in human macrophages: a novel link between cholesterol metabolism and inflammation. PLoS ONE 2010;5(7):e11765. doi: https://doi.org/10.1371/journal.pone.0011765.
[15] Reboldi A, Dang EV, McDonald JG, Liang G, Russell DW, Cyster JG, et al. 25-Hydroxycholesterol suppresses interleukin-1-driven inflammation downstream of type I interferon. Science 2014;345:679–84. doi: https://doi.org/10.1126/science.1254790.
[16] Blanc M, Hsieh WY, Robertson KA, Watterson S, Shui G, Lacaze P, et al. Host defense against viral infection involves interferon mediated down-regulation of sterol biosynthesis. PLoS Biol 2011;9(3):e1000598. doi: https://doi.org/10.1371/journal.pbio.1000598.
[17] Chen Y, Zhu J, Lum PY, Yang X, Pinto S, MacNeil DJ, et al. Variations in DNA elucidate molecular networks that cause disease. Nature 2008;452(7186):429–35. doi: https://doi.org/10.1038/nature06757.
[18] Bauman DR, Bitmansour AD, McDonald JG, Thompson BM, Liang G, Russell DW. 25-Hydroxycholesterol secreted by macrophages in response to Toll-like receptor activation suppresses immunoglobulin A production. Proc Natl Acad Sci USA 2009;106(39):16764–9. doi: https://doi.org/10.1073/pnas.0909142106.
[19] Gold ES, Diercks AH, Podolsky I, Podyminogin RL, Askovich PS, Treuting PM, et al. 25-Hydroxycholesterol acts as an amplifier of inflammatory signaling. Proc Natl Acad Sci USA 2014;111(29):10666–71. doi: https://doi.org/10.1073/pnas.1404271111.
[20] Diczfalusy U, Olofsson KE, Carlsson A-M, Gong M, Golenbock DT, Rooyackers O, et al. Marked upregulation of cholesterol 25-hydroxylase expression by lipopolysaccharide. J Lipid Res 2009;50(11):2258–64. doi: https://doi.org/10.1194/jlr.M900107-JLR200.

[21] Liu S-Y, Aliyari R, Chikere K, Li G, Marsden M, Smith J, et al. Interferon-inducible cholesterol-25-hydroxylase broadly inhibits viral entry by production of 25-hydroxycholesterol. Immunity 2013;38(1):92–105. doi: https://doi.org/10.1016/j.immuni.2012.11.005.
[22] Liu Y, Wei Z, Ma X, Yang X, Chen Y, Sun L, et al. 25-Hydroxycholesterol activates the expression of cholesterol 25-hydroxylase in an LXR-dependent mechanism. J Lipid Res 2018;59(3):439–51. doi: https://doi.org/10.1194/jlr.M080440.
[23] Lumeng CN, Bodzin JL, Saltiel AR. Obesity induces a phenotypic switch in adipose tissue macrophage polarization. J Clin Invest 2007;117(1):175–84. doi: https://doi.org/10.1172/JCI29881.
[24] Jiang SY, Yang X, Yang Z, Li JW, Xu MQ, Qu YX, et al. Discovery of an insulin-induced gene binding compound that ameliorates nonalcoholic steatohepatitis by inhibiting sterol regulatory element-binding protein-mediated lipogenesis. Hepatology 2022. doi: https://doi.org/10.1002/hep.32381.
[25] Liang G, Yang J, Horton JD, Hammer RE, Goldstein JL, Brown MS. Diminished hepatic response to fasting/refeeding and liver X receptor agonists in mice with selective deficiency of sterol regulatory element-binding protein-1c. J Biol Chem 2002;277(11):9520–8. doi: https://doi.org/10.1074/jbc.M111421200.
[26] Zhang H, Wei Q, Tsushima H, Puviindran V, Tang YJ, Pathmanapan S, et al. Intracellular cholesterol biosynthesis in enchondroma and chondrosarcoma. JCI Insight 2019;4(11). doi: https://doi.org/10.1172/jci.insight.127232.
[27] Im SS, Yousef L, Blaschitz C, Liu J, Edwards R, Young S, et al. Linking lipid metabolism to the innate immune response in macrophages through sterol regulatory element binding protein-1a. Cell Metab 2011;13(5):540–9. doi: https://doi.org/10.1016/j.cmet.2011.04.001.
[28] Sag D, Cekic C, Wu R, Linden J, Hedrick CC. The cholesterol transporter ABCG1 links cholesterol homeostasis and tumour immunity. Nat Commun 2015;6:6354. doi: https://doi.org/10.1038/ncomms7354.
[29] Dang EV, McDonald JG, Russell DW, Cyster JG. Oxysterol Restraint of Cholesterol Synthesis Prevents AIM2 Inflammasome Activation. Cell 2017;171(5):1057–1071.e11. doi: https://doi.org/10.1016/j.cell.2017.09.029.
[30] Kratz M, Coats B, Hisert K, Hagman D, Mutskov V, Peris E, et al. Metabolic dysfunction drives a mechanistically distinct proinflammatory phenotype in adipose tissue macrophages. Cell Metab 2014;20(4):614–25. doi: https://doi.org/10.1016/j.cmet.2014.08.010.
[31] Moon YA, Liang G, Xie X, Frank-Kamenetsky M, Fitzgerald K, Koteliansky V, et al. The Scap/SREBP pathway is essential for developing diabetic fatty liver and carbohydrate-induced hypertriglyceridemia in animals. Cell Metab 2012;15(2):240–6. doi: https://doi.org/10.1016/j.cmet.2011.12.017.
[32] Hamilton JA. Colony-stimulating factors in inflammation and autoimmunity. Nat Rev Immunol 2008;8(7):533–44. doi: https://doi.org/10.1038/nri2356.
[33] Mehrpouri M, Bashash D, Mohammadi MH, Gheydari ME, Satlsar ES, Hamidpour M. Co-culture of Platelets with Monocytes Induced M2 Macrophage Polarization and Formation of Foam Cells: Shedding Light on the Crucial Role of Platelets in Monocyte Differentiation. Turk J Haematol 2019;36:97–105. doi: https://doi.org/10.4274/tjh.galenos.2019.2018.0449.
[34] Ivashkiv LB. IFNgamma: signalling, epigenetics and roles in immunity, metabolism, disease and cancer immunotherapy. Nat Rev Immunol 2018;18:545–58. doi: https://doi.org/10.1038/s41577-018-0029-z.
[35] Zhu L, Zhao Q, Yang T, Ding W, Zhao Y. Cellular metabolism and macrophage functional polarization. Int Rev Immunol 2015;34(1):82–100. doi: https://doi.org/10.3109/08830185.2014.969421.
[36] Joseph SB, Castrillo A, Laffitte BA, Mangelsdorf DJ, Tontonoz P. Reciprocal regulation of inflammation and lipid metabolism by liver X receptors. Nat Med 2003;9(2):213–9. doi: https://doi.org/10.1038/nm820.
[37] Dahlman I, Nilsson M, Gu HF, Lecoeur C, Efendic S, Östenson CG, et al. Functional and genetic analysis in type 2 diabetes of liver X receptor alleles–a cohort study. BMC Med Genet 2009;10(1). doi: https://doi.org/10.1186/1471-2350-10-27.
[38] Solaas K, Legry V, Retterstol K, Berg PR, Holven KB, Ferrieres J, et al. Suggestive evidence of associations between liver X receptor beta polymorphisms with type 2 diabetes mellitus and obesity in three cohort studies: HUNT2 (Norway), MONICA (France) and HELENA (Europe). BMC Med Genet 2010;11:144. doi: https://doi.org/10.1186/1471-2350-11-144.
[39] Kalaany NY, Gauthier KC, Zavacki AM, Mammen PPA, Kitazume T, Peterson JA, et al. LXRs regulate the balance between fat storage and oxidation. Cell Metab 2005;1(4):231–44. doi: https://doi.org/10.1016/j.cmet.2005.03.001.
[40] Korach-Andre M, Parini P, Larsson L, Arner A, Steffensen KR, Gustafsson JA. Separate and overlapping metabolic functions of LXRalpha and LXRbeta in C57Bl/6 female mice. Am J Physiol Endocrinol Metab 2010;298:E167–178. doi: https://doi.org/10.1152/ajpendo.00184.2009.
[41] Bidault G, Virtue S, Petkevicius K, Jolin HE, Dugourd A, Guénantin AC, et al. SREBP1-induced fatty acid synthesis depletes macrophages antioxidant defences to promote their alternative activation. Nat Metab 2021;3(9):1150–62. doi: https://doi.org/10.1038/s42255-021-00440-5.